



Graphene intercalated with carbon nanosphere: a novel solid-phase extraction sorbent for five carbamate pesticides

Liyang Guo¹ · Jingyu Wu¹ · Fei Xing¹ · Weihua Liu¹ · Lin Hao¹ · Chun Wang¹ · Qiuhua Wu¹ · Zhi Wang¹

Received: 3 April 2020 / Accepted: 18 August 2020 / Published online: 27 August 2020
© Springer-Verlag GmbH Austria, part of Springer Nature 2020

Abstract

Graphene-carbon nanosphere composite (G@CNS) was prepared via a simple hydrothermal method. The G@CNS nanocomposite was characterized by X-ray diffraction, scanning electron microscope, surface area, and porosity analysis. The G@CNS was applied as a new sorbent for solid-phase extraction of five carbamate pesticides (tsumacide, carbaryl, isoprocab, bassa, diethofencarb) prior to quantitative determination by high-performance liquid chromatography with ultraviolet detection at 208 nm. Some experimental parameters including desorption conditions, sample pH, sample volume, and loading rate were studied carefully. Under the optimized condition, the method provided good linearity ranging from 0.3 to 100.0 ng mL⁻¹ with low limits of detection of 0.10–0.20 ng mL⁻¹ for grape juice, 0.10–0.30 ng mL⁻¹ for blend fruit juice, and 0.10–0.20 ng mL⁻¹ for water sample. Good method recoveries (80.2–110%) with relative standard deviations less than 7.2% and high enrichment factors (167–293) were achieved. Results demonstrated that this novel G@CNS can serve as a promising alternative sorbent for more applications.

Keywords Graphene · Carbon nanospheres · Solid-phase extraction · Carbamates · High-performance liquid chromatography

Introduction

The use of pesticides is a conventional agricultural practice worldwide to increase farming yield. Carbamate insecticides are water-soluble insecticides widely used in agricultural production. However, some adverse effects on human and environment are associated with their extensive use. Carbamates are toxic to the nervous system because they can inhibit acetylcholinesterase activity [1]. More importantly, carbamates are suspected carcinogens and mutagens [2]. Many countries or organizations, such as The European and The US Environmental Protection Agency (EPA), have established controls for their use and set maximum residue limits for them

(5–200 µg kg⁻¹) [3]. Therefore, the determination of carbamate residues in foodstuffs and environmental samples at trace levels is very important for human health and environmental protection.

As most of carbamates are thermally unstable, the most commonly preferred determination technique for them is high-performance liquid chromatography (HPLC) coupled with different detectors like ultraviolet [4], photodiode array [5], or mass spectrometry [6]. In most instances, the carbamate residual concentration in real samples is very low, and real samples often have very complex matrices, which make most real samples unsuitable for direct analysis. Therefore, to eliminate the analytical uncertainties and ensure a reliable determination of carbamates, sample preparation is a very important step in analysis process. Many sample pretreatment methods have been developed for pre-concentration and separation of carbamates from sample matrix, such as solid-phase microextraction (SPME) [7], liquid-phase microextraction (LPME) [8], dispersive liquid-liquid microextraction (DLLME, a variant of LPME) [9], solid-phase extraction (SPE) [10, 11], and magnetic solid-phase extraction (MSPE, a variant of SPE) [12]. Among them, SPE, a well-developed commercialized sample preparation technique, has been widely adopted in trace analysis due to its good repeatability, low consumption of organic solvents, and high enrichment factors.

Electronic supplementary material The online version of this article (<https://doi.org/10.1007/s00604-020-04497-z>) contains supplementary material, which is available to authorized users.

✉ Chun Wang
wangchun@hebau.edu.cn

✉ Qiuhua Wu
qiuhuawu@126.com

¹ College of Science, Hebei Agricultural University, Baoding 071001, China

In SPE, the choice of an appropriate and highly efficient sorbent is a key factor for achieving high enrichment efficiency. Since the commercially available SPE sorbents are still limited, researches are currently focused on the development and the applications of novel materials as SPE sorbents. Carbon-based materials are well-known to be good sorbents due to their excellent sorption ability and low cost. Carbon-based materials have been thoroughly explored and have undergone significant evolution, from activated carbon [13], carbon nanotubes [14], to graphene (G) [15]. They have been playing increasingly important roles in numerous scientific and technical fields. Up to now, plenty of carbon-based nanomaterials, involving fullerenes [16], carbon nanotubes [17], and graphene (G) [2], as well as their functionalized forms, have been investigated as adsorbent materials in sample preparation. Graphene, a carbon material with 2D “aromatic” monolayer of carbon atoms structure, has attracted extensive attention because it has good mechanical properties, optical properties, and large adsorption ability. Due to these properties, graphene has been widely used in many applications such as electrochemical biosensing [18], sorbent for organic pollutants [19], removal of metal ions [20], and catalyst support [21]. However, graphene is prone to irreversible aggregation due to strong van der Waals forces and strong hydrophobic property [22]. Thus, many approaches have been adopted to prevent restacking of graphene sheets. A simple strategy is the intercalation of nanosized spacers, such as carbon black [23], carbon nanotubes [24], and carbon spheres [25]. A recent report has confirmed that using carbon nanospheres (CNS) to modify graphene can effectively prevent graphene from restacking [26]. Compared with CNS-free graphene counterpart, the resulting composite has been applied as electrode materials, showing a high capacitance values and excellent rate capabilities. Considering that carbon materials have good sorption ability, intercalating carbon nanospheres into graphene sheets will integrate the strong sorption ability of both the graphene and carbon nanospheres, resulting in an advanced sorbent. But no study was reported for exploring the sorption performance of such a graphene-carbon nanosphere material.

In continuation of our previous work for exploring new carbon-based materials as adsorbent in sample preparation [27, 28], in this work, a graphene-carbon nanosphere (G@CNS) composite was synthesized. Five carbamates (tsumacide, carbaryl, isoprocarb, bassa, diethofencarb) are commonly used in local area, and their residues will pose risks to human health and environment. Thus, they were selected as the model analytes to evaluate the adsorption performance of G@CNS by employing it as the SPE adsorbent. Their sorption performance was also compared with some commercialized sorbents. Finally, a sensitive method was developed by combining the G@CNS-based SPE technique with HPLC-ultraviolet detection, and

successfully applied to determine five carbamate pesticides in juice and reservoir water samples.

Experimental

Chemicals and materials

Tsumacide, carbaryl, isoprocarb, bassa, and diethofencarb were purchased from Aladdin Reagent (Shanghai, China, <http://www.aladdin-e.com>), and their structures are given in Fig. S1 in the electronic supplementary materials (ESM). Acetone, acetonitrile, and methanol were HPLC-grade and were supplied by Huaxin Chemical Regent Company. Graphite powder (320 meshes) was purchased from the Boaixin Chemical Reagents Company (Baoding, China). KMnO_4 , H_2O_2 (30%), H_3PO_4 (85%) and concentrated H_2SO_4 (95–98%) were purchased from Kaitong Chemical Reagent (Tianjin, China). Glucose and sodium chloride were purchased from Macklin Reagent (Shanghai, China <http://www.macklin.cn>). Juice samples were purchased from local supermarket, and water samples were taken from local reservoir.

The standard stock solutions containing five carbamates each at $40.0 \mu\text{g mL}^{-1}$ were prepared in volumetric flask with methanol as solvent and stored in the dark at 4°C . The standard working solution was freshly prepared by diluting the stock solution with methanol.

Instrumentation

The chromatographic analysis was performed on an Agilent Technologies 1260 Infinity LC that consists of a binary solvent delivery pump, an ultraviolet detector, a manual injector, and OpenLAB CDS ChemStation software. Separation was conducted on a C18 column ($250 \text{ mm} \times 4.6 \text{ mm ID}$, $5.0 \mu\text{m}$) purchased from Dalian Johnsson Separation Science Technology Corporation (Dalian, China). The mobile phase was a mixture of acetonitrile-water (48:52, v/v) at a flow rate of 1 mL min^{-1} for grape juice, acetonitrile-water (44:56, v/v) at a flow rate of 1 mL min^{-1} for reservoir water and blend fruit juice. The injection volume was $20 \mu\text{L}$, and the detection wavelength was chosen at 208 nm.

X-ray diffraction (XRD) measurements were carried out using a Bruker D8 ADVANC (Bruker, Germany). The nitrogen adsorption isotherm (77.3 K) and surface area were measured on V-Sorb 2008P surface area and pore size distribution analyzer (Jinaipu, China <http://app-one.cnpowder.com.cn>). S-4800 Scanning Electron Microscope (SEM) (Hitachi, Japan) was used to characterize the graphene oxide and reduced graphene-carbon nanosphere material. The infrared spectra (IR) were performed with a WQF-510 IR spectrometer (Ruili, China).

Synthesis of G@CNS

Synthesis of graphene oxide

Graphene oxide (GO) was prepared from natural graphite powders by modified Hummers method [29]. A 9:1 mixture of concentrated $\text{H}_2\text{SO}_4/\text{H}_3\text{PO}_4$ (1000:111 mL) was added to a mixture of graphite flakes (10.0 g) and KMnO_4 (54.0 g). The reaction was then heated to 50 °C and stirred for 12 h. After cooled to room temperature, the mixture was poured onto ice, followed by adding 30% H_2O_2 (10 mL). When the color of the solution turned to yellow from dark brown, the mixture was centrifuged and washed sequentially with 1:10 HCl aqueous solution, 10% NaCl aqueous solution, and water until the pH was 7. The obtained GO aqueous dispersion was then sonicated for 60 min to obtain exfoliated GO with lamellar structure. After removing water by a rotary evaporator, vacuum freeze-drying process was conducted to obtain the GO product.

Synthesis of carbon nanosphere

Carbon nanosphere (CNS) was prepared by hydrothermal carbonization of glucose. Two grams of glucose dissolved in 18 mL of water was transferred to an autoclave. The autoclave was heated at 180 °C for 24 h, and then the product was washed with distilled water and isopropanol, respectively. After drying the product at 80 °C overnight, CNS was finally obtained.

Synthesis of G@CNS

G@CNS was synthesized by hydrothermal reduction and self-assembly of a GO aqueous dispersion in the presence of a certain amount of CNS according to the literature with some modifications [25]. Sixty milliliters of the GO aqueous dispersion (1 mg mL^{-1}) was mixed with 180 mg CNS. The mixture was sonicated for 30 min and then transferred to an autoclave. The reaction was carried out at 200 °C for 24 h, followed by washing with distilled water and methanol, respectively. After drying at 80 °C overnight, G@CNS composite was finally obtained.

For comparison, G@CNS_1 and G@CNS_2 were prepared by the same strategy except that 115 mg CNS and 45 mg CNS were added, respectively. G was prepared using the same procedure without adding CNS.

Sample preparation

Reservoir water and juice samples were separately filtered through 0.45- μm membrane to remove the suspended particulates. Fifty milliliters of filtered juice sample was diluted to 100 mL with ultrapure water and then used for the following SPE.

SPE cartridge preparation and SPE procedure

To prepare the SPE cartridge, 25 mg G@CNS was weighed and packed into a 3-mL empty SPE cartridge between two sieve plates. The packed cartridge was first conditioned with 3 mL methanol, 3 mL acetonitrile, and 3 mL ultrapure water. Then 100-mL sample solution was passed through the cartridge at 2 mL min^{-1} . After that, the cartridge was washed with 5 mL 1:10 acetonitrile aqueous solution to remove some interference from matrixes. Then, the carbamates adsorbed in the G@CNS were eluted with 300 μL of methanol, and obtained eluate was analyzed by the HPLC.

Results and discussion

Characterization of G@CNS

The G@CNS was characterized by specific surface and pore size analysis, XRD, IR, and scanning electron microscope, respectively. The XRD pattern of GO and G@CNS is shown in Fig. 1a. GO displayed a sharp diffraction (001) peak at 2θ of ca. 12°, corresponding to the *c*-axis interlayer distance (*d*-spacing) of 0.76 nm between randomly stacked GO layers. For G@CNS, the characteristic diffraction peak of GO at about 12° disappeared and a broad peak at about 25° corresponding to the (002) reflection of graphene appeared, indicating that GO was reduced to G under the hydrothermal reduction condition [30]. The broad 002 reflection suggested the poor ordering of G sheets along their stacking direction.

Figure 1b displays the FTIR spectra of GO and G@CNS. The spectrum of GO demonstrated the existence of oxygen-containing functional moieties in GO. The broad band at 3423 cm^{-1} can be assigned to O–H stretching vibration. The band at 1654 cm^{-1} can be assigned to aromatic C=C. The band at 1080 cm^{-1} and 1727 cm^{-1} can be attributed to C–O and C=O stretching vibration, respectively, in carboxylic acid and carbonyl moieties. However, for the G@CNS, all these absorption peaks related to the oxidized groups almost disappeared in the FT-IR spectrum, demonstrating the reduction of the above-mentioned functional groups.

Nitrogen adsorption-desorption isotherm and pore size distribution of G@CNS in Fig. 1c exhibit that the G@CNS possessed a microporous and mesoporous structure. The Brunauer-Emmett-Teller (BET) specific surface area of G@CNS is 59.8 $\text{m}^2 \text{g}^{-1}$, and single point adsorption total pore volume is 0.0595 $\text{cm}^3 \text{g}^{-1}$. The SEM images in Fig. 1d show that G owned lamellar structure with some aggregation. CNS displayed a spherical structure with relatively smooth and uniform surface and the CNS size is about 5 μm (Fig. 1e). From the SEM image of G@CNS in Fig. 1f, it can be clearly seen that the spherical CNS is intercalated within the interlayer spaces of the G.

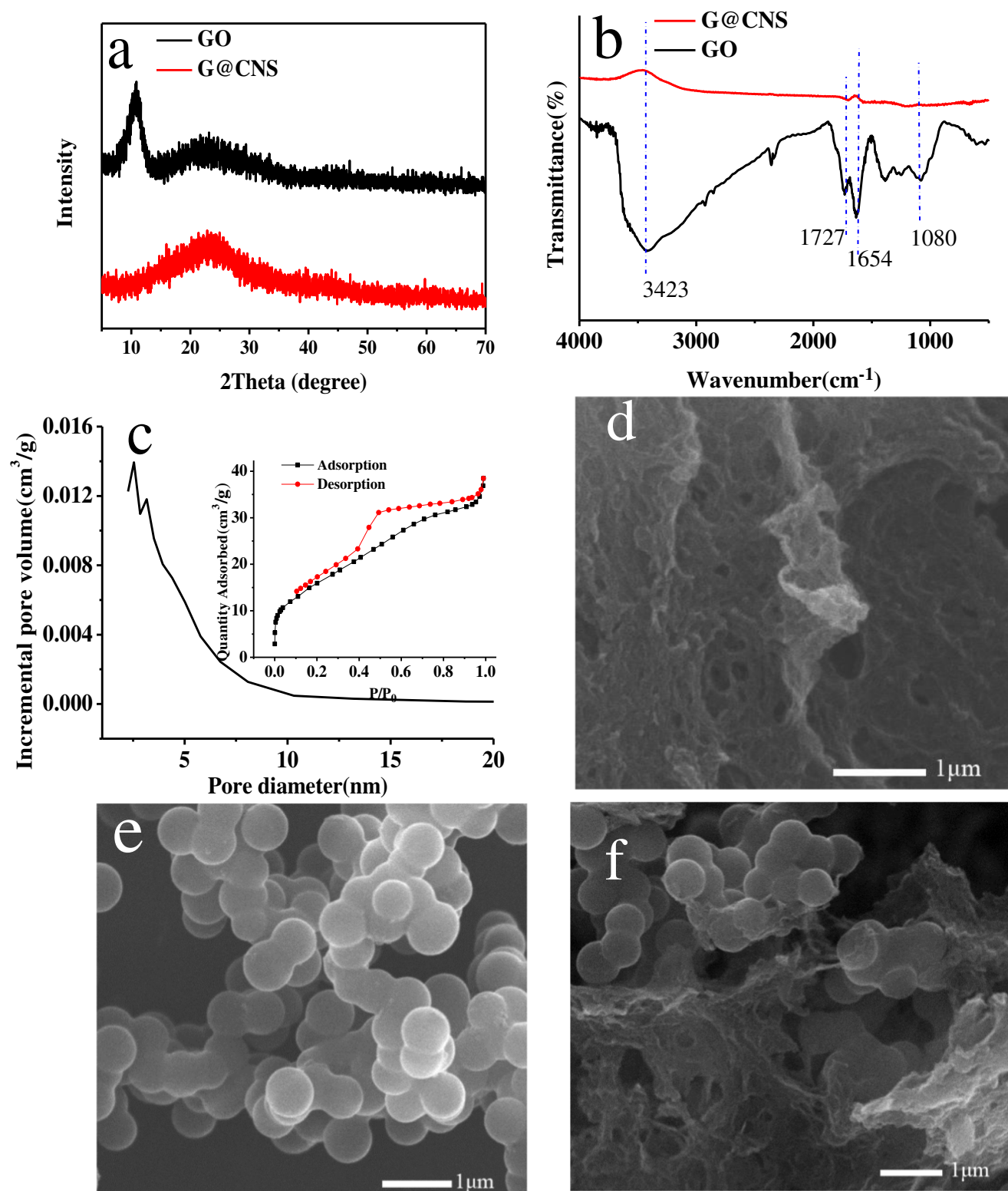


Fig. 1 The XRD (a) and IR spectra (b) of GO and G@CNS, N₂ adsorption-desorption isotherms of G@CNS, SEM image of G (d), CNS (e), G@CNS (f)

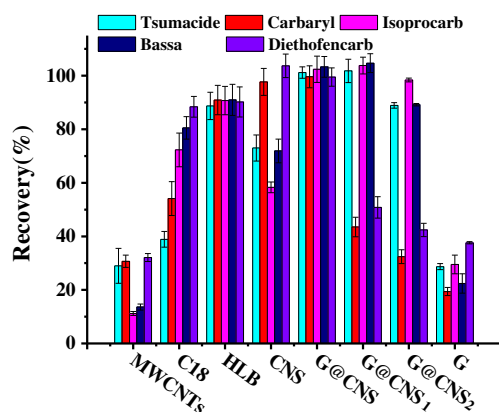


Fig. 2 Sorption comparison of different sorbents

Sorption performance

To evaluate the sorption performance of G@CNS adsorbent, the adsorption capacity of G@CNS with different CNS contents was studied, and their extraction efficiency was compared with its parent counterpart and several commonly used commercialized sorbent including C18, MWCNTs, and HLB (Hydrophilic-Lipophilic Balance) SPE adsorbent under their respective optimal conditions determined by preliminary experiments. In this regard, same amount of each sorbent (25 mg) was packed into a 3-mL cartridge in the same way. After 100 mL water solution containing 40 ng mL⁻¹ of each carbamate pesticide was loaded onto the cartridge, 1.2 mL methanol was used to completely elute the carbamates. Among the three commercialized sorbent, HLB as an acknowledged SPE adsorbent for carbamates showed the best sorption performance with extraction recovery about 90% (Fig. 2). Among all the tested sorbents, the G@CNS displayed the best sorption ability to five carbamates with extraction recovery (about 100%), greatly higher than that of G and CNS, slightly higher than that of HLB. The result proved that G@CNS can serve as a good sorbent for sensitive determination of trace carbamates. In addition, the adsorption efficiency of G is very low, probably due to the restacking of G sheets. In G@CNS, both the CNS and G played roles for the adsorption of carbamates, but CNS was also served as a spacer between G sheets to prevent the G aggregation thus improving adsorption performance. Compared with that of G@CNS₁ and G@CNS₂, there are more CNS intercalated into graphene sheets in G@CNS, effectively preventing the restacking of graphene, thereby achieving good adsorption.

Optimization of solid-phase extraction conditions

In order to guarantee high extraction efficiency, the effect of different experimental conditions on extraction performance was checked, involving the elution solvent and elution

volume, pH, volume of loading sample, and sample loading rate. The initial experimental conditions are as follows: 100-mL sample; spiked concentration of 40.0 ng mL⁻¹; sample pH = 6; loading rate of 2 mL min⁻¹; 1.2 mL methanol as elution solvent. Univariate approach was used for the optimization, i.e., when a single factor was varied, the others were fixed. Three parallel experiments were performed for each parameter. To ensure reliable results, the adsorbent was not reused during optimization steps.

Optimization of elution solvent and elution volume

Different elution solvents have different elution power for target analytes, resulting different elution performances. Desorption of the carbamates from the G@CNS sorbents was studied by using different type organic solvents (acetonitrile, methanol, acetone). Figure S2 shows that among the three solvents tested, methanol provided the highest recovery. As a result, methanol was chosen as the desorption solvent in the following experiments.

In addition, volume of the eluent is also an important parameter influencing the desorption efficiency, so different methanol volumes of 0.3, 0.6, 0.9, 1.2, and 1.5 mL were studied. From the results in Fig. S3, with the increase of the eluent volume, the recoveries were improved, but the recoveries changed very little with the further increase in methanol volume up to 1.2 mL. This result suggests that 1.2 mL methanol is needed to completely desorb carbamates from the G@CNS adsorbents. However, using larger volume of eluent volume will reduce the detection sensitivity due to the dilution effect (Fig. S4). Thus, for a higher sensitivity, 0.3 mL methanol was used as eluent volume. Before the next use, the G@CNS packed SPE cartridge was washed with 2 mL methanol and 2 mL water to ensure no carryover.

Optimization of pH

Most carbamates are instable and easier to hydrolyze in alkaline solution, which can affect its extraction efficiency. In this study, the effect of pH upon carbamate extractability in G@CNS-based SPE was tested by varying the sample solution pH from 2 to 10. From the results shown in Fig. S5, good extraction efficiency for five of the carbamates was observed at pH 2–6. At higher pH, and especially at alkaline conditions, except diethofencarb, other four carbamates showed significantly decreased in the recovery due to the hydrolysis. Since the pH of real samples in this work is between 4 and 6, there is no need to change pH.

Optimization of volume of loading sample

The optimum volume of loading sample is a vital parameter affecting enrichment factor and sensitivity of the method. To

investigate the influence of sample volume, sample solution of 50–170 mL was passed through the cartridge. From the results shown in Fig. S6, it can be found that when the sample loading volume is below 100 mL, the recoveries of the studied compounds all maintained at high levels. However, when the volume is over 100 mL, it was observed a decrease in the recovery values with increasing sample volumes. Considering both the enrichment factor and sensitivity, 100-mL sample volume was adopted.

Optimization of sample loading rate

Another important parameter that may affect both analysis time and extraction efficiency of the SPE is the flow rate. Different loading rates will lead to a great difference in the loading time of the sample, and may affect the pre-concentration efficiency. Flow rates of 1, 2, 3, and 4 mL min⁻¹ were studied respectively. From the results shown in Fig. S7, at a flow rate of less than 2 mL min⁻¹, there was no significant change in recovery. But the recovery decreased sharply when flow rate was higher than 2 mL min⁻¹. Therefore, 2 mL min⁻¹ was selected in the analysis.

In summary, the optimal conditions are as follows: sample volume: 100 mL; sample loading rate: 2 mL min⁻¹; no adjustment of the pH; the desorption conditions: 0.3 mL methanol.

Preparation reproducibility

To investigate the batch-to-batch reproducibility of the synthesis procedure, the G@CNS materials were prepared in three different batches, and then they were characterized by FT-IR

and XRD, respectively. The results displayed that the FT-IR and XRD patterns of the G@CNS from the three batches were consistent (Fig. S8). Then, the G@CNS materials were used for SPE of the carbamates. The extraction recoveries of the carbamates were almost the same (Fig. S9), indicating that the preparation of the materials was reproducible.

Reusability of adsorbent

Whether the adsorbent can be reused is one of the important criteria for its practical applications. The reusability of G@CNS was also evaluated. Prior to the next cycle, the used SPE column was washed with 1 mL (0.5 × 2) of methanol and 1 mL of water to ensure no carry-over of the carbamates. The G@CNS SPE column can be reused for 25 times without significant loss of its adsorption performance (Fig. S10), demonstrating its excellent reusability.

Evaluation of the method

In order to assess the proposed method, determination coefficient (R^2), studied linear range (LR), relative standard deviation (RSD), limits of detection (LODs), and limits of quantification (LOQs) were evaluated using the optimized extraction conditions. In order to eliminate the possible matrix effects, all calibration plots are established using matrix-matched spiked samples. For this purpose, a series of standard solution with different concentrations were added to the analytes-free blank samples to finally obtain a series of spiked samples (0.3, 2.0, 10.0, 20.0, 40.0, and 100.0 ng mL⁻¹). The analytical data obtained are presented in Table 1. Over the range of 0.3–

Table 1 Linear range, LODs, LOQs, and precision data for the target compounds of the method coupled with HPLC

Samples	Carbamates	Linear range (ng mL ⁻¹)	LODs (ng mL ⁻¹)	LOQs (ng mL ⁻¹)	R^2	RSDs (%)	EF
Reservoir water	Tsumacide	0.3–100.0	0.10	0.30	0.9994	6.3	264
	Carbaryl	0.3–100.0	0.10	0.30	0.9998	4.7	181
	Isoprocarb	0.3–100.0	0.10	0.30	0.9998	4.1	260
	Bassa	0.6–100.0	0.20	0.60	0.9992	3.9	293
	Diethofencarb	0.3–100.0	0.10	0.30	0.9998	4.4	223
Grape juice	Tsumacide	0.3–100.0	0.10	0.30	0.9974	4.1	252
	Carbaryl	0.3–100.0	0.10	0.30	0.9998	5.2	172
	Isoprocarb	0.3–100.0	0.10	0.30	0.9996	3.6	258
	Bassa	0.6–100.0	0.20	0.60	0.9948	2.8	275
	Diethofencarb	0.3–100.0	0.10	0.30	0.9964	2.3	217
Blend fruit juice	Tsumacide	1.0–100.0	0.30	1.0	0.9967	2.8	225
	Carbaryl	0.3–100.0	0.10	0.30	0.9964	3.0	167
	Isoprocarb	0.6–100.0	0.20	0.60	0.9992	6.7	235
	Bassa	1.0–100.0	0.30	1.0	0.9995	5.9	277
	Diethofencarb	0.6–100.0	0.20	0.60	0.9918	7.2	209

100.0 ng mL⁻¹, most carbamates exhibited good linearity, with R^2 ranging from 0.9992 to 0.9998 for reservoir water, 0.9964 to 0.9998 for grape juice, and 0.9918 to 0.9995 for blend fruit juice, respectively. The LODs, based on signal-to-noise ratio (S/N) of 3, were 0.10–0.20 ng mL⁻¹ for reservoir water, 0.10–0.20 ng mL⁻¹ for grape juice, and 0.10–0.30 ng mL⁻¹ for blend fruit juice, respectively. LOQ, the minimum concentration that can be quantitatively determined, were 0.30–0.60 ng mL⁻¹ for reservoir water, 0.30–0.60 ng mL⁻¹ for grape juice, and 0.30–1.0 ng mL⁻¹ for blend fruit juice. The repeatability of the method was determined by analyzing five parallel analyses of the samples spiked with each of the carbamates at 0.6 ng mL⁻¹ for reservoir water and grape juice sample, 2.0 ng mL⁻¹ for blend fruit juice, respectively. RSD values were between 3.9 and 6.3% for reservoir water sample, 2.3 and 5.2% for grape juice, and 2.8 and 7.2% for blend fruit juice. Enrichment factor (EF) of the carbamate, defined as the ratio of the carbamates concentration in the final eluate to that in the initial sample solution, was 167–293.

Application in real sample

The newly developed G@CNS-based SPE coupled with HPLC technique was applied to determine the five carbamates in water taken from local reservoir, and grape juice

and blend fruit juice purchased from local market. The results showed that 0.35 ng mL⁻¹ tsumacide was detected in grape juice, and carbaryl was detected in grape juice at a concentration lower than its LOQ. For blend fruit juice, isoproc carb was detected at a concentration lower than its LOQ. These samples were spiked with each analyte at two levels to check the accuracy of the method. As shown in Table 2, the method recoveries of five carbamates were in the range of 80.7–103% with RSD between 2.1 and 5.8% for reservoir water samples, 80.2–109% with RSD between 2.3 and 5.3% for grape juice, and 82.9–110% with RSD between 3.7 and 7.5% for blend fruit juice sample. The typical chromatograms of reservoir water, grape juice, and blend fruit juice before and after being spiked with the five carbamates are shown in Fig. 3.

Possible adsorption mechanism

Intermolecular forces mainly include van-der-Waals forces, hydrophobic interactions, hydrogen bonds, and π - π stacking interactions. As G possesses large delocalized π -electron system, which can form strong π -stacking interaction with the benzene ring, the π - π stacking interactions between the G@CNS and carbamates played a greater role for the adsorption. Moreover, owing to the strong hydrophobicity of the G@CNS, hydrophobic interactions also made some contribution to the

Table 2 Results for the analysis of real samples and the recovery study in spiked samples

Carbamates	Spiked (ng mL ⁻¹)	Reservoir water			Grape Juice				Blend fruit juice			
		Found (ng mL ⁻¹)	MR (%)	RSDs (%)	Spiked (ng mL ⁻¹)	Found (ng mL ⁻¹)	MR (%)	RSDs (%)	Spiked (ng mL ⁻¹)	Found (ng mL ⁻¹)	MR (%)	RSDs (%)
Tsumacide	0.0	nd			0.0	0.35			0.0	nd		
	0.6	0.54	89.3	2.1	0.6	0.58	97.1	3.4	2.00	2.09	104	4.2
	1.5	1.29	86.2	4.2	2.0	2.13	106	2.2	6.00	6.55	109	7.5
Carbaryl	0.0	nd			0.0	< LOQ			0.0	nd		
	0.6	0.51	85.5	5.6	0.6	0.48	80.2	4.1	2.00	1.68	84.2	3.7
	1.5	1.52	101	4.5	2.0	2.06	102	4.7	6.00	4.22	70.3	6.3
Isoproc carb	0.0	nd			0.0	0.8			0.0	< LOQ		
	0.6	0.48	80.7	5.3	0.6	0.59	98.2	4.9	2.00	2.21	110	4.5
	1.5	1.48	98.6	4.9	2.0	2.15	107	3.8	6.00	6.14	102	4.1
Bassa	0.0	nd			0.0	nd			0.0	nd		
	0.6	0.59	98.8	3.5	0.6	0.52	85.9	2.3	2.00	1.74	87.1	6.2
	1.5	1.32	87.8	5.8	2.0	1.82	91.1	4.3	6.00	4.81	80.2	4.0
Diethofencarb	0.0	nd			0.0	nd			0.0	nd		
	0.6	0.62	103	2.4	0.6	0.61	105	3.1	2.00	2.18	109	3.8
	1.5	1.25	83.6	3.7	2.0	2.19	109	5.3	6.00	6.08	101	6.3

MR, method recovery; nd, not detected. The found concentration values in the table are the values after deducting the concentration in the corresponding blank sample

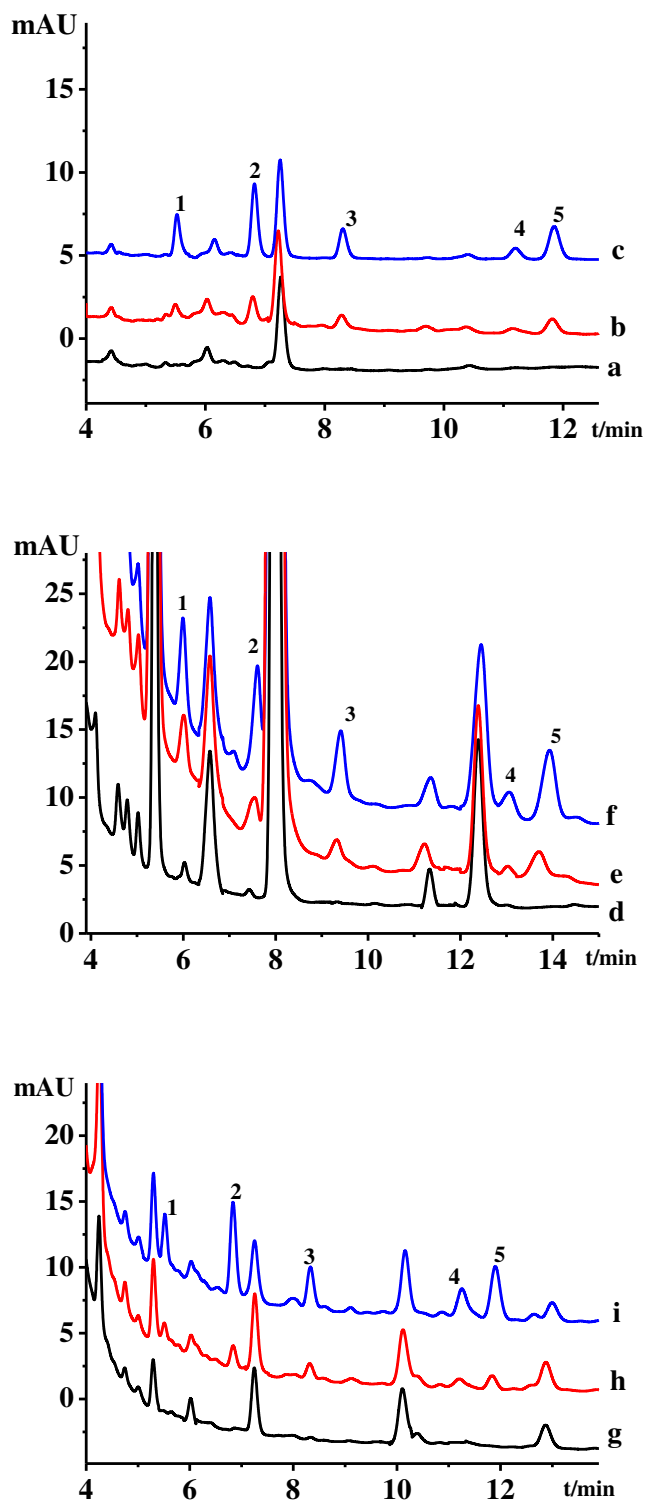


Fig. 3 Typical HPLC-UV chromatograms of reservoir water sample (a); reservoir water sample spiked with carbamates at each concentration of 0.6 ng mL^{-1} and 1.5 ng mL^{-1} (b, c); grape juice sample (d); grape juice sample spiked with carbamates at each concentration of 0.6 ng mL^{-1} and 2 ng mL^{-1} (e, f); blend fruit juice sample (g); blend fruit juice sample spiked with carbamates at each concentration of 2 ng mL^{-1} and 6 ng mL^{-1} (h, i). Peaks: 1, tsumacide; 2, carbaryl; 3, isoprocarb; 4, bassa; and 5, diethofencarb

adsorption. Hence, G@CNS may be a good candidate as an adsorbent for the adsorption of benzenoid compounds through hydrophobic interactions and π - π stacking interactions. The organic pollutants containing benzenoid structures, such as many herbicides, pesticides, fungicides, and PAHs, can be adsorbed by G@CNS. So, it is a good adsorbent for the adsorption of compounds with aromatic ring.

Method comparison

The proposed method for the analysis of carbamates in juice samples and water sample was compared with other different methods. The results in Table 3 demonstrated that the LOD of proposed method is comparable with that of MSA-DLLME-HPLC-DAD [31] and SPE-HPLC-DAD method [32], and much lower than that of other methods [33–37], indicating a higher sensitivity of the proposed method. Although the LOD of MSPE-HPLC-MS [6], PT-SPE-UHPLC-MS [38], and mPFC-UPLC-MS method [39] is lower than that of the developed method, MS detector is sensitive detection technique, which is more expensive and less available for routine analysis. From the viewpoint of extraction time, the proposed method required a much shorter time to reach adsorption equilibrium than SPME-LC-MS [36], LLE-LTP-HPLC-UV [34], and MMF-SPME-HPLC-DAD [40]. In comparison with MEPS-HPLC-UV [35], MSA-DLLME-HPLC-DAD [31], and MSPE-HPLC-UV [33], the extraction time of proposed method is relatively long, but SPE technique has the advantages of easier use than the MEPS, MSA-DLLME, and MSPE methods. These results confirmed that the proposed method is relatively simple and sensitive.

Conclusion

In the current study, a series of G@CNS nanocomposites with different CNS contents were successfully synthesized through a simple hydrothermal strategy. G@CNS₁ nanocomposites displayed a superior sorption ability toward carbamate pesticides compared with G@CNS₂, G@CNS₃, and some commercial sorbents. Combined the G@CNS-based SPE with HPLC-UV technique, a method for determination of carbamates in juice and water samples was proposed for the trace level analysis of carbamates in water and juice samples. Result indicated that the G@CNS can serve as a superior SPE adsorbent, and the current SPE-HPLC-UV method is expected to have more applications in analysis field. The adsorption selectivity of G@CNS is relatively poor and future work should be focused on functional modification to improve the selectivity.

Table 3 Comparison with other methods for carbamate analysis

Sample preparation methods	Detection	Sample	Linear range	LODs	Extraction (min)	Carbamates in common	Ref
MSA-DLLME	HPLC-DAD	Tea drinks	1–1000 $\mu\text{g mL}^{-1}$	0.13–0.61 ng mL^{-1}	5	Carbaryl	[31]
SPE	HPLC-DAD	Juice	1.0–80.0 ng mL^{-1}	0.2–0.3 ng mL^{-1}	20	Isoprocarb	[32]
MSPE	HPLC-UV	Tomatoes	5–200 ng g^{-1}	0.58–2.06 ng g^{-1}	20	Isoprocarb	[33]
LLE-LTP	HPLC-UV	River water	0.33–500 mg L^{-1}	5–10 ng mL^{-1}	180	Carbaryl, isoprocarb	[34]
MEPS	HPLC-UV	Juice	0.5–200 ng mL^{-1}	0.23–1.21 ng mL^{-1}	8	Carbaryl, isoprocarb, diethofencarb	[35]
SPME	LC-MS	Juice	/	5–50 ng mL^{-1}	90	Diethofencarb	[36]
SPE	HPLC-UV	Benincasahispida	1.0–40.0 ng g^{-1}	0.3–0.5 ng g^{-1}	33	Carbaryl, isoprocarb, diethofencarb	[37]
PT-SPE	UHPLC-MS	Juice	0.012–10 ng mL^{-1}	0.0022–0.033 ng mL^{-1}	12	Isoprocarb, diethofencarb	[38]
mPFC	UPLC-MS	Vegetables	1–50 ng mL^{-1}	0.02–1.5 $\mu\text{g kg}^{-1}$	1	Tsumacide, carbaryl, isoprocarb, diethofencarb	[39]
MMF-SPME	HPLC-DAD	Water	0.1–200 $\mu\text{g L}^{-1}$	0.017–0.29 $\mu\text{g L}^{-1}$	50	Carbaryl, isoprocarb	[40]
MSPE	HPLC-MS	Juice	0.2–80 ng mL^{-1}	0.04–0.30 ng mL^{-1}	20	Carbaryl, isoprocarb, diethofencarb	[6]
SPE	HPLC-UV	Juice	1–100 ng mL^{-1}	0.1–0.3 ng mL^{-1}	50	Tsumacide, carbaryl, isoprocarb, bassa, diethofencarb	This work
		Reservoir water	1–100 ng mL^{-1}	0.1–0.2 ng mL^{-1}			

MSA-DLLME, magnetic stirring-assisted dispersive liquid-liquid microextraction; LLE-LTP, liquid-liquid extraction with low temperature partitioning; c:MEPS, microextraction in a packed syringe; d:PT-SPE, pipette tip solid-phase extraction; mPFC, multi-plug filtration cleanup; MMF-SPME, multiple monolithic fiber solid-phase microextraction

Funding information Financial supports from the National Natural Science Foundation of China (31471643, 31571925, 31671930), the Natural Science Foundation of Hebei Province (B2020204001, C2020204020, C2020204136, B2017204025, C2018204076), the Preferential Foundation for the Introduction of Overseas Scholars by Hebei Province (CL201713), and the Natural Science Foundation of Hebei Agricultural University (LG201607, LG201610, ZD201703, LG201712, LG201806) are gratefully acknowledged.

Compliance with ethical standards

Conflict of interest The authors declare that they have no conflict of interest.

Ethical approval This article does not contain any studies with human or animal subjects.

Informed consent Not applicable.

References

- Worek F, Aurbek N, Wetherell J, Pearce P, Mann T, Thiermann H (2008) Inhibition, reactivation and aging kinetics of highly toxic organophosphorus compounds: pig versus minipig acetylcholinesterase. *Toxicology* 244:35–41. <https://doi.org/10.1016/j.tox.2007.10.021>
- Shi Z, Hu J, Li Q, Zhang S, Liang Y, Zhang H (2014) Graphene based solid phase extraction combined with ultra high performance liquid chromatography-tandem mass spectrometry for carbamate pesticides analysis in environmental water samples. *J Chromatogr A* 1355:219–227. <https://doi.org/10.1016/j.chroma.2014.05.085>
- Moreno-González D, Huertas-Pérez JF, Gámiz-Gracia L, García-Campaña AM (2015) High-throughput methodology for the determination of 33 carbamates in herbal products by UHPLC–MS/MS. *Food Anal Methods* 8:2059–2068. <https://doi.org/10.1007/s12161-014-9998-0>
- Khodadoust S, Talebianpoor MS, Ghaedi M (2014) Application of an optimized dispersive nanomaterial ultrasound-assisted microextraction method for preconcentration of carbofuran and propoxur and their determination by high-performance liquid chromatography with UV detection. *J Sep Sci* 37:3117–3124. <https://doi.org/10.1002/jssc.201400816>
- Wang X, Meng X, Wu Q, Wang C, Wang Z (2019) Solid phase extraction of carbamate pesticides with porous organic polymer as adsorbent followed by high performance liquid chromatography-diode array detection. *J Chromatogr A* 1600:9–16. <https://doi.org/10.1016/j.chroma.2019.04.031>
- Wang X, Feng T, Wang J, Hao L, Wang C, Wu Q, Wang Z (2019) Preparation of magnetic porous covalent triazine-based organic polymer for the extraction of carbamates prior to high performance liquid chromatography-mass spectrometric detection. *J Chromatogr A* 1602:178–187. <https://doi.org/10.1016/j.chroma.2019.06.046>
- Zhou J, Ma C, Zhou S, Ma P, Chen F, Qi Y, Chen H (2010) Preparation, evaluation and application of molecularly imprinted solid-phase microextraction monolith for selective extraction of pirimicarb in tomato and pear. *J Chromatogr A* 1217:7478–7483. <https://doi.org/10.1016/j.chroma.2010.09.079>
- Farajzadeh MA, Sorouraddin SM, Mogaddam MRA (2014) Liquid phase microextraction of pesticides: a review on current methods.

- Microchim Acta 181:829–851. <https://doi.org/10.1007/s00604-013-1157-6>
9. Yang E-Y, Shin H-S (2013) Trace level determinations of carbamate pesticides in surface water by gas chromatography–mass spectrometry after derivatization with 9-xanthidrol. *J Chromatogr A* 1305: 328–332. <https://doi.org/10.1016/j.chroma.2013.07.055>
 10. Mena ML, Martínez-Ruiz P, Reviejo AJ, Pingarrón JM (2002) Molecularly imprinted polymers for on-line preconcentration by solid phase extraction of pirimicarb in water samples. *Anal Chim Acta* 451:297–304. [https://doi.org/10.1016/S0003-2670\(01\)01421-0](https://doi.org/10.1016/S0003-2670(01)01421-0)
 11. Moreno-González D, Huertas-Pérez JF, García-Campaña AM, Gámiz-Gracia L (2014) Determination of carbamates in edible vegetable oils by ultra-high performance liquid chromatography–tandem mass spectrometry using a new clean-up based on zirconia for QuEChERS methodology. *Talanta* 128:299–304. <https://doi.org/10.1016/j.talanta.2014.04.045>
 12. Wu Q, Zhao G, Feng C, Wang C, Wang Z (2011) Preparation of a graphene-based magnetic nanocomposite for the extraction of carbamate pesticides from environmental water samples. *J Chromatogr A* 1218:7936–7942. <https://doi.org/10.1016/j.chroma.2011.09.027>
 13. Sircar S, Golden TC, Rao MB (1996) Activated carbon for gas separation and storage. *Carbon* 34:1–12. [https://doi.org/10.1016/0008-6223\(95\)00128-X](https://doi.org/10.1016/0008-6223(95)00128-X)
 14. Pan B, Xing B (2008) Adsorption mechanisms of organic chemicals on carbon nanotubes. *Environ Sci Technol* 42:9005–9013. <https://doi.org/10.1021/es801777n>
 15. Xu J, Wang L, Zhu Y (2012) Decontamination of Bisphenol A from aqueous solution by graphene adsorption. *Langmuir* 28:8418–8425. <https://doi.org/10.1021/la301476p>
 16. Rodriguez JA, Ibarra IS, Miranda JM, Barrado E, Santos EM (2016) Magnetic solid phase extraction based on fullerene and activated carbon adsorbents for determination of azo dyes in water samples by capillary electrophoresis. *Anal Methods* 8:8466–8473. <https://doi.org/10.1039/C6AY02631A>
 17. Latrous El Atrache L, Hachani M, Kefi BB (2015) Carbon nanotubes as solid-phase extraction sorbents for the extraction of carbamate insecticides from environmental waters. *Int J Environ Sci Technol* 13:201–208. <https://doi.org/10.1007/s13762-015-0861-7>
 18. Wang Y, Shao Y, Matson DW, Li J, Lin Y (2010) Nitrogen-doped graphene and its application in electrochemical biosensing. *ACS Nano* 4:1790–1798. <https://doi.org/10.1021/nn100315s>
 19. Ma X, Wang J, Wu Q, Wang C, Wang Z (2014) Extraction of carbamate pesticides in fruit samples by graphene reinforced hollow fibre liquid microextraction followed by high performance liquid chromatographic detection. *Food Chem* 157:119–124. <https://doi.org/10.1016/j.foodchem.2014.02.007>
 20. Yusuf M, Elfgi FM, Zaidi SA, Abdullah EC, Khan MA (2015) Applications of graphene and its derivatives as an adsorbent for heavy metal and dye removal: a systematic and comprehensive overview. *RSC Adv* 5:50392–50420. <https://doi.org/10.1039/c5ra07223a>
 21. Imran Jafri R, Rajalakshmi N, Ramaprabhu S (2010) Nitrogen doped graphene nanoplatelets as catalyst support for oxygen reduction reaction in proton exchange membrane fuel cell. *J Mater Chem* 20:7114–7117. <https://doi.org/10.1039/C0JM00467G>
 22. Hou X, Tang S, Wang J (2019) Recent advances and applications of graphene-based extraction materials in food safety. *TrAC Trends Anal Chem* 119:115603. <https://doi.org/10.1016/j.trac.2019.07.014>
 23. Yan J, Wei T, Shao B, Ma F, Fan Z, Zhang M, Zheng C, Shang Y, Qian W, Wei F (2010) Electrochemical properties of graphene nanosheet/carbon black composites as electrodes for supercapacitors. *Carbon* 48:1731–1737. <https://doi.org/10.1016/j.carbon.2010.01.014>
 24. Yu D, Dai L (2010) Self-assembled graphene/carbon nanotube hybrid films for supercapacitors. *J Phys Chem Lett* 1:467–470. <https://doi.org/10.1021/jz9003137>
 25. Guo CX, Li CM (2011) A self-assembled hierarchical nanostructure comprising carbon spheres and graphene nanosheets for enhanced supercapacitor performance. *Energy Environ Sci* 4:4504. <https://doi.org/10.1039/c1ee01676h>
 26. Díez N, Qiao M, Gómez-Urbano JL, Botas C, Carriazo D, Titirici MM (2019) High density graphene-carbon nanosphere films for capacitive energy storage. *J Mater Chem A* 7:6126–6133. <https://doi.org/10.1039/c8ta12050a>
 27. Guo L, Hao L, Gao T, Wang C, Wu Q, Wang Z (2019) p-Phenylenediamine-modified graphene oxide as a sorbent for solid-phase extraction of phenylurea herbicides, nitroimidazoles, chlorophenols, phenylurea insecticides and phthalates. *Microchim Acta* 186:464. <https://doi.org/10.1007/s00604-019-3606-3>
 28. Sun M, Tang R, Wu Q, Wang C, Wang Z (2014) Graphene reinforced hollow fiber liquid phase microextraction for the enrichment of some phenylurea residues in milk sample. *Food Anal Methods* 7: 1097–1102. <https://doi.org/10.1007/s12161-013-9719-0>
 29. Marcano DC, Kosynkin DV, Berlin JM, Sinitiskii A, Sun Z, Slesarev A, Alemany LB, Lu W, Tour JM (2010) Improved synthesis of graphene oxide. *ACS Nano* 4:4806–4814. <https://doi.org/10.1021/nn1006368>
 30. Tang Z, Zhang Z, Han Z, Shen S, Li J, Yang J (2016) One-step synthesis of hydrophobic-reduced graphene oxide and its oil/water separation performance. *J Mater Sci* 51:8791–8798. <https://doi.org/10.1007/s10853-016-9937-0>
 31. Wang X, Cheng J, Zhou H, Wang X, Cheng M (2013) Development of a simple combining apparatus to perform a magnetic stirring-assisted dispersive liquid-liquid microextraction and its application for the analysis of carbamate and organophosphorus pesticides in tea drinks. *Anal Chim Acta* 787:71–77. <https://doi.org/10.1016/j.aca.2013.05.033>
 32. Wu J, Liang X, Hao L, Wang C, Wu Q, Wang Z (2017) Graphene oxide cross-linked with phytic acid: an efficient adsorbent for the extraction of carbamates. *Microchim Acta* 184:3773–3779. <https://doi.org/10.1007/s00604-017-2413-y>
 33. Li N, Chen J, Shi YP (2015) Magnetic graphene solid-phase extraction for the determination of carbamate pesticides in tomatoes coupled with high performance liquid chromatography. *Talanta* 141:212–219. <https://doi.org/10.1016/j.talanta.2015.04.018>
 34. Goulart SM, Alves RD, Neves AA, de Queiroz JH, de Assis TC, de Queiroz ME (2010) Optimization and validation of liquid-liquid extraction with low temperature partitioning for determination of carbamates in water. *Anal Chim Acta* 671:41–47. <https://doi.org/10.1016/j.aca.2010.05.003>
 35. Sun T, Fan Y, Fan P, Geng F, Chen P, Zhao F (2019) Use of graphene coated with ZnO nanocomposites for microextraction in packed syringe of carbamate pesticides from juice samples. *J Sep Sci* 42:2131–2139. <https://doi.org/10.1002/jssc.201900257>
 36. Sagratini G, Manes J, Giardina D, Damiani P, Pico Y (2007) Analysis of carbamate and phenylurea pesticide residues in fruit juices by solid-phase microextraction and liquid chromatography–mass spectrometry. *J Chromatogr A* 1147:135–143. <https://doi.org/10.1016/j.chroma.2007.02.066>
 37. Gao T, Wang J, Wu Q, Wang C, Wang Z (2019) A graphene oxide-based composite for solid-phase extraction of carbamate pesticides from vegetables. *Food Anal Methods* 13:690–698. <https://doi.org/10.1007/s12161-019-01685-3>
 38. Shi Z, Li Q, Xu D, Huai Q, Zhang H (2016) Graphene-based pipette tip solid-phase extraction with ultra-high performance liquid chromatography and tandem mass spectrometry for the analysis of carbamate pesticide residues in fruit juice. *J Sep Sci* 39:4391–4397. <https://doi.org/10.1002/jssc.201600498>